Improving the spatial distribution of modeled Arctic sea ice thickness

Article

Published Version

Improving the spatial distribution of modeled Arctic sea ice thickness

Paul A. Miller, Seymour W. Laxon, and Daniel L. Feltham

Centre for Polar Observation and Modelling, Department of Space and Climate Physics, University College London, London, UK

Received 10 June 2005; revised 8 July 2005; accepted 9 August 2005; published 28 September 2005.

[1] The spatial distribution of ice thickness/draft in the Arctic Ocean is examined using a sea ice model. A comparison of model predictions with submarine observations of sea ice draft made during cruises between 1987 and 1997 reveals that the model has the same deficiencies found in previous studies, namely ice that is too thick in the Beaufort Sea and too thin near the North Pole. We find that increasing the large scale shear strength of the sea ice leads to substantial improvements in the model's spatial distribution of sea ice thickness, and simultaneously improves the agreement between modeled and ERS-derived 1993–2001 mean winter ice thickness. **Citation:** Miller, P. A., S. W. Laxon, and D. L. Feltham (2005), Improving the spatial distribution of modeled Arctic sea ice thickness, *Geophys. Res. Lett.*, *32*, L18503, doi:10.1029/2005GL023622.

1. Introduction

[2] A number of studies have shown that the Arctic sea ice cover has changed substantially in recent decades. Decreases in sea ice extent since the early 1980s [*Parkinson and Cavalieri*, 2002] and substantial thinning derived from analyses of sparse submarine measurements of ice draft [*Rothrock et al.*, 1999] both point to a sea ice cover undergoing rapid change.

[3] In seeking to understand the factors responsible for the apparent thinning, models are used for hindcast simulations of Arctic sea ice thickness [*Rothrock et al.*, 2003]. But whether contemporary sea ice models are sufficiently accurate to have confidence in their thickness predictions is still open to question. *Rothrock et al.* [2003] compared predictions from various published studies of Arctic ice thickness over the last 50 years and highlighted the substantial disagreement among the models used (their Figure 12).

[4] Confidence in model predictions can be increased by assessing their agreement with observations of Arctic sea ice that have become available in recent years. *Rothrock et al.* [2003] compared their coupled ice-ocean model to measurements of Arctic sea ice draft taken on 9 winter and summer submarine cruises between 1987 and 1997. Despite good agreement with Arctic averaged drafts, they found substantial disagreement between their model and the observed spatial pattern in the ice draft/thickness field (their Figure 9), with modeled ice thicker than observed in the Beaufort Sea and thinner near the North Pole.

[5] Here we examine this discrepancy using the Los Alamos sea ice model, CICE [*Hunke and Lipscomb*, 2001]. However, we use the optimized CICE model with parameters previously optimized through comparison with satellite observations of sea ice extent, speed statistics and thickness [*Miller et al.*, 2005]. Comparing model output to the same ice draft data sets as used by *Rothrock et al.* [2003], we investigate the spatial discrepancy they observed to determine whether it can be reduced while maintaining agreement with satellite observations of sea ice extent, speed statistics and thickness.

0094-8276/05/2005GL023622$05.00

2. Model and Forcing

[6] CICE [*Hunke and Lipscomb*, 2001] has energy-conserving thermodynamics [*Bitz and Lipscomb*, 1999], an elastic-viscous-plastic (EVP) rheology [*Hunke and Dukowicz*, 1997], and an explicit parameterization of ridging that transfers sea ice between five thickness categories in response to local rates of strain [*Flato and Hibler*, 1995].

[7] Atmospheric forcing consists of six-hourly 10-meter winds, snowfall, and longwave and shortwave radiation taken from the ECMWF's ERA-40 reanalysis, and daily 2-meter temperatures from the POLES/IABP data set. A simple mixed layer model is used to calculate oceanic heat flux, and ice-ocean drag is calculated using spatially varying, temporally constant ocean currents [*Zhang et al.*, 1998].

[8] The model is run on a rotated latitude-longitude grid with a resolution of 1°, and is spun-up for 12 years using 1980 forcing repeatedly, after which it simulates Arctic sea ice from 1980 to 2001.

[9] CICE was tuned by varying the ice strength parameter, P^* [*Hibler*, 1979], the air drag parameter, C_a, and the albedo of cold, thick ice, α, and analyzing the output from multiple runs to identify a set of these parameter values with which the model output most closely agreed with satellite observations of sea ice thickness [*Laxon et al.*, 2003], extent (calculated from sea ice concentration data [*Cavalieri et al.*, 2002]) and speed statistics (calculated using the monthly sea ice velocity fields of *Fowler* [2003]) for the years 1993 to 2001 [*Miller et al.*, 2005]. The optimal parameter set was found to be $\{\alpha, C_a, P^*\} = \{0.56, 0.0006, 5\ \mathrm{kN\ m^{-2}}\}$, values that lie within commonly-used ranges [e.g., *Hibler*, 1979; *Rothrock et al.*, 2003].

3. Comparing Modeled and Observed Draft

[10] To compare modeled ice draft to submarine ice draft we use the same digitally-recorded ULS draft data from 9 submarine cruises between 1987 and 1997 used by *Rothrock et al.* [2003, Figure 4]. The data for this mix of winter and summer cruises is available from the NSIDC with Cruise Reference Names: UK-87 (Superb), 1988a, UK-91, 1991, L2-92, SCICEX-93, 1994, SCICEX-96, and SCICEX-97. We use 860 linear sections with lengths that vary from 10 km to 65 km.

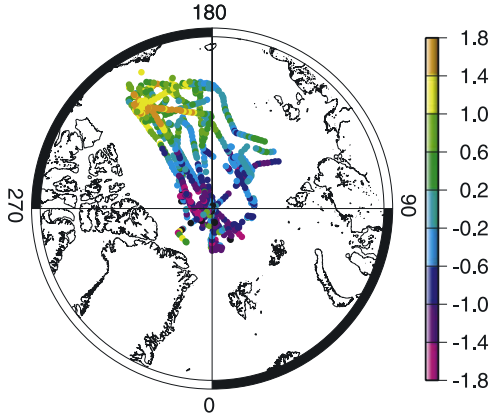

Figure 1. Modeled minus observed mean draft (m) for all cruise tracks between 1987 and 1997, for the model with $e = 2$.

[11] Figure 1 shows modeled minus observed draft for all 860 sections (RMS = 0.93 m, $R = 0.54$). The similarity to *Rothrock et al.* [2003, Figure 9] is striking. Modeled ice in both cases is too thick in the Beaufort Sea and too thin near the North Pole. Moreover, an examination of ice draft output for models run with a range of commonly-used parameter values ($\alpha \in [0.56, 0.66]$, $C_a \in [0.0006, 0.0016]$ and $P^* \in [5, 27.5]$ kN m^{-2}) revealed that this discrepancy was persistent, and not a consequence of the particular parameters chosen.

[12] Apart from the 2-meter temperature field, the data used to force the two models are different. Also, *Rothrock et al.* [2003] use a coupled ice-ocean model with a higher, 40 km resolution and a more complex ice strength parameterization. This suggests that the spatial discrepancy is due to one or more of the dynamical parameterizations shared by the models, e.g. the viscous-plastic (VP) rheology with an elliptical yield curve and a ratio of major to minor axes, $e = 2$ [*Hibler*, 1979], or the ice thickness redistribution due to ridging. In fact, *Kreyscher et al.* [2000] also found that a model with a VP rheology and an elliptical yield curve ($e = 2$) predicted ice in the Beaufort Sea over 1.5 m thicker than observed. Similarly, *Fichefet and Morales Maqueda* [1997] found that modeled annually-averaged ice thickness increased by 1.5 m in the Canadian Basin and decreased by similar amounts near the North Pole when shear strength was neglected. The evidence therefore suggests that the large scale shear strength of the ice in the model has a significant influence on the spatial distribution of modeled sea ice.

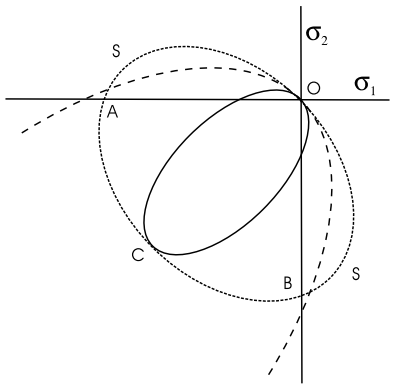

Figure 2. Elliptical yield curves used for the EVP rheology, where σ_1 and σ_2 are the principal stresses. Solid yield curve: $P^* = 7.5$ kN m^{-2} and the ratio of major to minor axes $e = 2$. Dotted yield curve: $P^* = 7.5$ kN m^{-2} and $e^2 = 0.5$. Curve OACBO: Truncated elliptical yield curve with $e^2 = 0.5$ and $P^* = 7.5$ kN m^{-2}. Dashed line: The commonly-used [*Hibler and Walsh*, 1982] yield curve with $e = 2$ and $P^* = 27.5$ kN m^{-2}.

4. Improvements Due to Increased Large Scale Shear Strength

[13] Increasing the shear strength of the ice in the model, so that the ice can withstand more shear stress before deforming plastically, can be accomplished by decreasing the ratio of the elliptical yield curve's major to minor axes, e. The value of $e = 2$ (solid ellipse in Figure 2) is widely used [*Hibler*, 1979; *Kreyscher et al.*, 2000; *Rothrock et al.*, 2003; *Miller et al.*, 2005] and was chosen on the basis of comparisons with ice deformation [*Hibler*, 1975, 1979].

[14] Since the evidence pointed to the need for increased shear strength in the model, we reduced e from its standard value and found that modeled ice draft decreased in the Beaufort Sea and simultaneously increased near the North Pole, improving the agreement between the modeled and observed spatial distributions. After adjusting model parameters to $\{\alpha, C_a, e^2, P^*\} = \{0.56, 0.00085, 0.5, 7.5 \text{ kN m}^{-2}\}$, we found close agreement between both modeled and observed ice drafts and speeds. Apart from e, these values are still within commonly-used ranges. The yield curve with $e^2 = 0.5$ is shown as the dotted ellipse in Figure 2.

[15] Figure 3 shows the improvement in the modeled minus observed draft when $e^2 = 0.5$ (RMS = 0.58 m, $R = 0.85$). The improvement can also be seen in Figure 4, where the modeled and observed zonal mean drafts agree much more closely for the model run with $e^2 = 0.5$ than the run with $e = 2$.

[16] Figure 5 shows the consequent improvement to the model's basin-scale thickness. With $e = 2$, the modeled mean 1993–2001 winter (November to April - ERS altim-

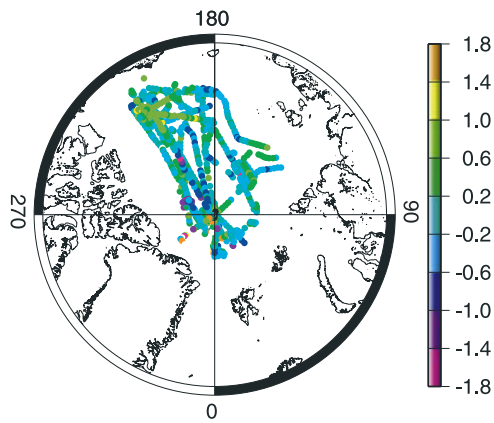

Figure 3. Modeled minus observed mean draft (m) for all cruise tracks between 1987 and 1997, for the model with $e^2 = 0.5$.

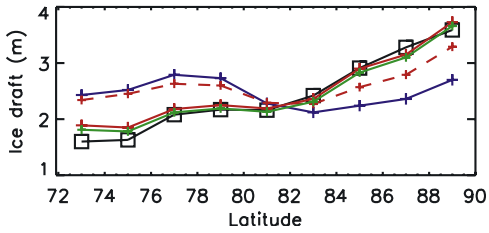

Figure 4. Mean draft in two-degree latitude bands from 72°N to 90°N. Black squares: observed; blue + symbol: $e = 2$: red + symbol: $e^2 = 0.5$; red dashed curve and + symbol: $e^2 = 0.5$, truncated; green curve and + symbol: $e^2 = 0.5$, truncated when ice concentration <0.8.

eter estimates of ice thickness are only available during the winter [*Laxon et al.*, 2003]) thickness field minus the ERS-observed field has a root mean square difference (RMS) of 0.55 m, and modeled ice is too thick in the Beaufort Sea and too thin in the Laptev and Kara Seas. The model run with $e^2 = 0.5$ has an improved spatial distribution (RMS = 0.44 m), and modeled ice thickness is more accurate in the Beaufort, Laptev and Kara Seas. However, since satellite-derived ice thickness data are not available above 81.5°N [*Laxon et al.*, 2003], further improvements to the spatial thickness distribution near the North Pole cannot be quantified.

5. Discussion and Conclusions

[17] As we have shown, increasing the large scale shear strength of modeled ice improves the spatial distribution of modeled ice draft. But why does increasing the shear strength have such an impact? Having a lower maximum shear strength, when $e = 2$ or higher for example, results in increased ridging and opening of leads for the strain rates close to shear observed in the Beaufort Gyre. Convergence in this region closes leads and ridges thinner ice until it becomes thick and compact enough to oppose further thickening, results in a reduced export of thick ice from the region, and allows thinner ice from elsewhere in the Arctic Ocean to be transported towards the North Pole to reduce average ice thickness there. Furthermore, the low shear strength allows thick ice from north of the Canadian Archipelago to be advected into the region. Conversely, a larger maximum shear strength ($e < 2$) results in less ridging and lead opening in the Beaufort Gyre, less convergence, greater export of thicker ice from the Beaufort Sea to the North Pole, and less advection of thick ice into the Beaufort Sea from north of the Canadian Archipelago.

[18] The interpretation of the new yield curve is that, whether diverging or converging, shear deformations require a larger shear stress than that predicted using the elliptical yield curve with $e = 2$. However, decreasing e also results in a continuum scale yield curve with appreciable tensile stress. This can be seen in Figure 2, where the yield curve with $e^2 = 0.5$ (dotted line) now has a more significant presence in the second and fourth quadrants of principal stress space than the curve with $e = 2$. However, for ice of a given ice thickness and concentration the size of the yield curve is determined by the ice strength parameter P^* [*Hibler*, 1979], and Figure 2 shows that for the yield curve with $e = 2$ and the commonly-used [*Hibler and Walsh*, 1982] value $P^* = 27.5$ kN m^{-2} (dashed curve), the tensile strength is similar to that of the new curve with $e^2 = 0.5$ and $P^* = 7.5$ kN m^{-2}.

[19] There is a great deal of legitimate uncertainty regarding the most appropriate representation of sea ice rheology on the continuum scale. Theoretical approaches can argue for various types of rheologies, including anisotropic rheologies [*Wilchinsky and Feltham*, 2004]. Though the adoption of a continuum-scale yield curve with appreciable tensile stress may be thought by some to be unphysical, the physics remains uncertain. *Coon et al.* [1998] measured tensile strength and found it to be non-zero, though small. Nor is the relationship between stresses in a lead to the continuum-scale yield curve straightforward. *Thorndike* [1987] argued that even in pure divergence the ice cover can have appreciable strength because of the non-monotonic relationship between continuum-scale strain rate and sub-continuum deformations. For example, although pure divergence may be occurring on the continuum scale, on the sub-continuum scale the individual floes and leads may be deforming quite differently.

[20] A particular concern with continuum-scale tensile strength is that it renders the resulting system of momentum and strain hardening/weakening equations unstable [*Gray*, 1999]. However, this instability is quite possibly a real phenomenon and may be responsible for the formation of linear kinematic features in the ice cover, as demonstrated in the recent work of *Hibler and Schulson* [2000].

[21] *Hopkins* [2001] investigated the effect of tensile strength on the continuum scale using a granular sea ice model and obtained very different yield curves in simulations depending on whether joints between floes were either unfrozen or frozen. In the former case, the yield curve was shown to be a near perfect tear drop shape with no tensile strength, whereas in the latter case, when tensile forces could be supported by the frozen joints, *Hopkins* [2001] obtained a broader, diamond-like shape with increased shear strength and some tensile strength.

[22] We altered the CICE code to truncate the $e^2 = 0.5$ yield curve and remove tensile strength, resulting in curve OACBO in Figure 2. The resulting zonal mean drafts are plotted in Figure 4 and are clearly worse than the untrun-

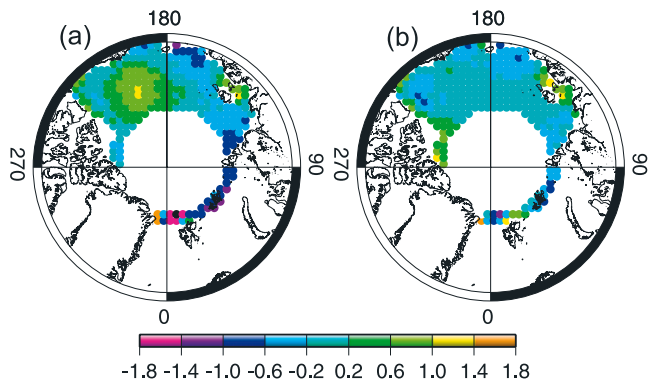

Figure 5. Modeled minus observed mean 1993–2001 winter thickness fields (m) for the model with (a) $e = 2$, and (b) $e^2 = 0.5$. Data are not available above 81.5°N [*Laxon et al.*, 2003].

cated case. However, drawing upon the work of *Hopkins* [2001] and truncating the yield curve only when the ice concentration is <0.8 to crudely parameterize the lack of frozen joints able to support tensile stress, we found that the modeled zonal mean drafts improved again (see Figure 4).

[23] Clearly, there many unanswered questions with regard to the most appropriate representation of sea ice rheology on the continuum scale. Nevertheless, we have shown here that a simple, physically reasonable change to the yield curve shape can improve the spatial distribution of modeled Arctic sea ice thickness. We hope that the improved agreement with observations of sea ice draft shown in this paper will help stimulate fresh thought on the matter. Until such time as better validated sea ice rheologies are introduced to continuum scale sea ice models, this simple change can be used to increase confidence in model predictions, which is important when using models to analyze the reasons for the substantial thinning observed in sparse submarine measurements of ice draft [*Rothrock et al.*, 1999] during the last 50 years.

[24] **Acknowledgments.** We are grateful to the model developers and to the Los Alamos National Laboratory for making CICE freely available to the scientific community. We thank the European Space Agency for the provision of the ERS data, the NSIDC for providing sea ice concentration and velocity data, the ECMWF for the ERA-40 reanalysis data, and the IABP/POLES teams for providing additional forcing data. The authors would like to thank two anonymous referees for their helpful comments. P.M. was funded by NERC through both the COAPEC thematic programme and the Centre for Polar Observation and Modelling.

References

Bitz, C. M., and W. H. Lipscomb (1999), An energy-conserving thermodynamic sea ice model for climate study, *J. Geophys. Res.*, *104*, 15,669–15,677.

Cavalieri, D. J., C. L. Parkinson, P. Gloersen, and H. J. Zwally (2002), Sea ice concentrations from Nimbus-7 SMMR and DMSP SSM/I passive microwave data [CD-ROM], http://nsidc.org/data/nsidc-0051.html, Natl. Snow and Ice Data Cent., Boulder, Colo.

Coon, M. D., G. S. Knoke, D. C. Echert, and R. S. Pritchard (1998), The architecture of an anisotropic elastic-plastic sea ice mechanics constitutive law, *J. Geophys. Res.*, *103*, 21,915–21,925.

Fichefet, T., and M. A. Morales Maqueda (1997), Sensitivity of a global sea ice model to the treatment of ice thermodynamics and dynamics, *J. Geophys. Res.*, *102*, 12,609–12,646.

Flato, G. M., and W. D. Hibler III (1995), Ridging and strength in modeling the thickness distribution of Arctic sea ice, *J. Geophys. Res.*, *100*, 18,611–18,626.

Fowler, C. (2003), Polar Pathfinder daily 25 km EASE-grid sea ice motion vectors, http://nsidc.org/data/nsidc-0116.html, Natl. Snow and Ice Data Cent., Boulder, Colo.

Gray, J. M. N. T. (1999), Loss of hyperbolicity and ill-posedness of the viscous-plastic sea ice rheology in uniaxial divergent flow, *J. Phys. Oceanogr.*, *29*, 2920–2929.

Hibler, W. D., III (1975), Differential sea-ice drift. II: Comparison of mesoscale strain measurements to linear drift theory predictions, *J. Glaciol.*, *13*, 457–471.

Hibler, W. D., III (1979), A dynamic-thermodynamic sea ice model, *J. Phys. Oceanogr.*, *9*, 815–846.

Hibler, W. D., III, and E. M. Schulson (2000), On modeling the anisotropic failure and flow of flawed sea ice, *J. Geophys. Res.*, *105*, 17,105–17,120.

Hibler, W. D., III, and J. E. Walsh (1982), On modeling the seasonal and interannual fluctuations of Arctic sea ice, *J. Phys. Oceanogr.*, *12*, 1514–1523.

Hopkins, M. A. (2001), The effect of tensile strength in the Arctic ice pack, in *IUTAM Symposium on Scaling Laws in Ice Mechanics and Ice Dynamics*, edited by J. P. Dempsey and H. H. Stern, pp. 373–386, Springer, New York.

Hunke, E. C., and J. K. Dukowicz (1997), An elastic-viscous-plastic model for sea ice dynamics, *J. Phys. Oceanogr.*, *27*, 1849–1867.

Hunke, E. C., and W. H. Lipscomb (2001), CICE: The Los Alamos Sea Ice Model, documentation and software user's manual, *LACC-98-16 v.3.*, Los Alamos Natl. Lab., Los Alamos, N. M. (Available at http://climate.lanl.gov/Models/CICE/index.htm)

Kreyscher, M., H. Harder, P. Lemke, and G. M. Flato (2000), Results of the Sea Ice Model Intercomparison Project: Evaluation of sea ice rheology schemes for use in climate simulations, *J. Geophys. Res.*, *105*, 11,299–11,320.

Laxon, S., N. Peacock, and D. Smith (2003), High interannual variability of sea ice thickness in the Arctic region, *Nature*, *425*, 947–950.

Miller, P. A., S. W. Laxon, D. L. Feltham, and D. J. Cresswell (2005), Optimization of a sea ice model using basin-wide observations of Arctic sea ice thickness, extent and velocity, *J. Clim.*, in press.

Parkinson, C. L., and D. J. Cavalieri (2002), A 21 year record of Arctic sea-ice extents, and their regional, seasonal and monthly variability and trends, *Ann. Glaciol.*, *34*, 441–446.

Rothrock, D. A., Y. Yu, and G. A. Maykut (1999), Thinning of the Arctic sea ice cover, *Geophys. Res. Lett.*, *26*, 3469–3472.

Rothrock, D., J. Zhang, and Y. Yu (2003), The Arctic ice thickness of the 1990s: A consistent view from observations and models, *J. Geophys. Res.*, *108*(C3), 3083, doi:10.1029/2001JC001208.

Thorndike, A. S. (1987), A random discontinuous model of sea ice motion, *J. Geophys. Res.*, *92*, 6515–6520.

Wilchinsky, A. V., and D. L. Feltham (2004), A continuum anisotropic model of sea ice dynamics, *Proc. R. Soc. London, Ser. A*, *460*, 2105–2140.

Zhang, J., D. Rothrock, and M. Steele (1998), Warming of the Arctic Ocean by a strengthened Atlantic inflow: Model results, *Geophys. Res. Lett.*, *25*, 1745–1748.

D. L. Feltham, S. W. Laxon, and P. A. Miller, Centre for Polar Observation and Modelling, Department of Space and Climate Physics, University College London, Gower Street, London, WC1E 6BT, UK. (swl@cpom.ucl.ac.uk)